

Distribution Embedding Networks for Generalization from a Diverse Set of Classification Tasks

Lang Liu^{1†} Mahdi Milani Fard² Sen Zhao²

¹ Department of Statistics, University of Washington

² Google Research

Abstract

We propose Distribution Embedding Networks (DEN) for classification with small data. In the same spirit of meta-learning, DEN learns from a diverse set of training tasks with the goal to generalize to unseen target tasks. Unlike existing approaches which require the inputs of training and target tasks to have the same dimension with possibly similar distributions, DEN allows training and target tasks to live in heterogeneous input spaces. This is especially useful for tabular-data tasks where labeled data from related tasks are scarce. DEN uses a three-block architecture: a covariate transformation block followed by a distribution embedding block and then a classification block. We provide theoretical insights to show that this architecture allows the embedding and classification blocks to be fixed after pre-training on a diverse set of tasks; only the covariate transformation block with relatively few parameters needs to be fine-tuned for each new task. To facilitate training, we also propose an approach to synthesize binary classification tasks, and demonstrate that DEN outperforms existing methods in a number of synthetic and real tasks in numerical studies.

1 Introduction

While machine learning has made substantial progress in many technological and scientific applications, its success often relies heavily on large-scale data. However, in many real-world problems, it is costly or even impossible to collect large training sets. For example, in online spam detection, at any time, we may only possess dozens of freshly labeled spam results. In health sciences, we may only have clinical outcomes on a few hundred study subjects. Few-shot learning (FSL) has recently been proposed as a new framework to tackle such small data problems. It has now gained huge attention in many applications such as image classification [17, 10], sentence completion [43, 31], and drug discovery [1]; see [46] for a survey.

The core idea behind most of FSL methods is to augment the limited training data with prior knowledge, e.g., images of other classes in image classification or similar molecules’ assays in drug discovery. In *meta-learning* based FSL, such prior knowledge is formulated as a set of related training tasks assumed to follow the same task distribution [10], with the goal that the trained model could quickly adapt to new tasks. In practice, however, given an arbitrary target task, the degree and nature of its relationship to the available auxiliary training data is often unknown. In this scenario, it is unclear if existing approaches can extract useful information from the training data and improve the performance on the target task. In fact, there is empirical evidence suggesting that learning from unrelated training tasks can lead to negative adaptation [7]. In our numerical studies, we also observe similar behavior; existing FSL approaches perform poorly when training tasks are unrelated to the target task.

In this paper, we investigate this important but under-studied setting—few-shot meta-learning with possibly unrelated tasks. We specifically focus on classification tasks with *tabular* data. Unlike machine

[†]Work done as an intern at Google Research.

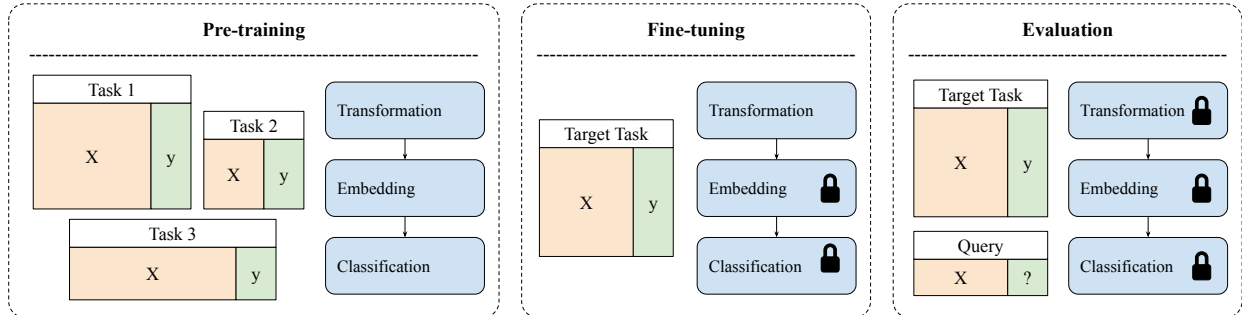


Figure 1: Training and evaluation of DEN. We first pre-train DEN on training tasks with heterogeneous covariate spaces. We then fine-tune the transformation block on a few labeled examples from the target task, and use the fine-tuned model for classification on the query set.

learning with image and text inputs, large datasets of related tasks are not available for generic tabular-data classification.

A key challenge in this setting is that the input, in the form of covariate vectors for training and target tasks, can live in different spaces and follow different distributions with possibly different dimensions. Existing meta-learning techniques often assume a *homogeneous* input space across tasks and thus cannot be directly applied in such cases with *heterogeneous* covariate spaces.

In this work, we propose Distribution Embedding Networks (DEN) for meta-learning on classification tasks with potentially *heterogeneous* covariate spaces. DEN consists of a novel three-block architecture. It first calibrates the raw covariates via a transformation block. A distribution embedding block is then applied to form an embedding vector serving as the “summary” of the target task. Finally, a classification block uses this task embedding vector along with the transformed query features to form a prediction.

Since the tasks can be unrelated, we learn a different transformation block for each task to form task-invariant covariates for the rest of the network. In other words, the transformation block is *task-dependent*. We keep the *task-independent* embedding and classification blocks fixed after *pre-training*, and use a few labeled examples from the target task (i.e., the support set) to *fine-tune* the task-dependent transformation block. Since our setting is significantly more challenging than the standard few-shot meta-learning setting due to the heterogeneity among training and target tasks, we assume that we have access to a slightly larger support set compared to the FSL setting (e.g., 50 examples in total across all classes rather than 5 examples per class). We further assume that the support set follows the same distribution as the query set. To address the challenge of variable-length covariates, the classification block is built upon a Deep Sets architecture [50]. Figure 1 shows an overview of the architecture and training and evaluation mechanisms.

To summarize our main contributions: (I) We propose a method for meta-learning with possibly unrelated tabular-data training tasks—an important setting that expands the application of meta-learning but has rarely been investigated in the literature; (II) We propose the three-block architecture, allowing the model to be pre-trained on a large variety of tasks, and then fine-tuned on an unrelated target task; we provide a scenario in which our three-block architecture can perform well; (III) Described in Section 5, we design a procedure to generate artificial tasks for pre-training, and empirically verify its effectiveness when testing on real tasks. This provides a principled way to generate training tasks and alleviates the cost of collecting real training tasks. (IV) We compare DEN with various existing FSL approaches on both simulated and real tasks, showing improved performance in most of the tasks we consider.

2 Related Work

There are multiple generic techniques applied to the meta-learning problem in the literature [46]. The first camp learns similarities between pairs of examples [17, 43, 2, 40, 33, 45, 41, 37, 27, 28]. For an unlabeled

example on a new task, we use its similarity score with labeled examples of the given task for classification. The second camp of optimization-based meta-learning aims to find a good starting point model such that it can quickly adapt to new tasks with a small number of labeled examples from the new task. This camp includes different variants of MAML [10, 23, 11, 13, 35] and Meta-Learner LSTM [34]. More recently, [21, 20] proposed to learn task-specific parameters for the loss weight and learning rate for out-of-distribution tasks. Their use of task-embedding is conceptually similar to DEN. The third camp is conceptually similar to topic modeling, such as Neural Statistician [9] and CNP [12], which learn a task specific (latent) embedding for classification. The final camp utilizes memory [36, 16, 30, 31]. Note that all the above methods assume that all training and target tasks are related and share the same input space.

A closely related problem is Domain Generalization (DG) which estimates a functional relationship between the input \mathbf{x} and output y given data from different domains (i.e., with different marginal $P(\mathbf{x})$); see, e.g., Wang et al. [44] and Zhou et al. [52] for surveys. The core idea lies behind a large class of DG methods is to learn a domain-invariant feature representation [see, e.g., 29, 24, 26, 38, 39], which aligns the marginal $P(\mathbf{x})$ and/or the conditional $P(y|\mathbf{x})$ distributions across multiple domains. In a similar spirit, DEN first adapts to the task via the transformation block and then learns a task-invariant representation via the task-independent embedding block.

Learning from heterogeneous feature spaces has been studied in transfer learning, or domain adaptation [5, 49, 8, 25, 48, 51]; see Day and Khoshgoftaar [6] for a survey. These approaches only focus on two tasks (source and target), and require the model to learn a transformation mapping to project the source and target tasks into the same space.

Unlike meta-learning and DG methods, DEN is applicable for tasks with *heterogeneous covariates spaces*. This phenomenon is especially prevalent in tabular data tasks, where the number and definition of features could be vastly different across tasks. Iwata and Kumagai [15] is among the first works that combine meta-learning with heterogeneous covariate spaces. Both their approach and DEN rely on pooling to handle variable-length inputs, using building blocks such as Deep Sets [50] and Set Transformers [22]. There are several differences between their approach and DEN. Firstly, DEN uses a covariate transformation block, allowing it adapt to new tasks more efficiently. Secondly, their model is permutation invariant in covariates and thus restrictive in model expressiveness; while DEN does not have this restriction. Thirdly, we also provide theoretical insights and justification for our model architecture design.

3 Notations

Let $\mathbb{T}_1, \dots, \mathbb{T}_M$ be M training tasks. For each training task \mathbb{T} , we observe an i.i.d. sample $\mathcal{D}_{\mathbb{T}} = \{(\mathbf{x}_{\mathbb{T},i}, y_{\mathbb{T},i})\}_{i \in [n_{\mathbb{T}}]}$ from some joint distribution $P_{\mathbb{T}}$, where $[n] = \{1, \dots, n\}$ and $\mathbf{x}_{\mathbb{T},i} \in \mathbb{R}^{d_{\mathbb{T}}}$ is the covariate vector of the i -th example and $y_{\mathbb{T},i} \in [L_{\mathbb{T}}]$ is its associated label. We denote this sample in matrix form by $(\mathbf{X}_{\mathbb{T}}, \mathbf{y}_{\mathbb{T}})$, where the j -th column $\mathbf{x}_{\mathbb{T}}^j \in \mathbb{R}^{n_{\mathbb{T}}}$ is the j -th covariate vector. We let $\mathbf{X}_{\mathbb{T},k}$ be the covariate sub-matrix corresponding to examples with label k for $k \in [L_{\mathbb{T}}]$. When the context is clear, we drop the dependency on \mathbb{T} for simplicity of the notation, e.g., we write $\mathbf{X}_{\mathbb{T},k}$ as \mathbf{X}_k .

Let \mathbb{S} be a target task that is not contained in the training tasks. We are given a set of labeled examples $(\mathbf{X}_{\mathbb{S}}, \mathbf{y}_{\mathbb{S}})$, where the sample size $n_{\mathbb{S}}$ is small. We refer to it as the *support set*. The goal is to predict labels for unlabeled examples in the target task, which is called the *query set*. We denote $\mathcal{T} = \{\mathbb{T}_1, \dots, \mathbb{T}_M, \mathbb{S}\}$.

4 Distribution Embedding Networks

We first describe the model architecture of DEN for binary classification in Section 4.1, and then extend DEN for multi-class classification in Section 4.2. Finally, we provide insights into the model architecture and justify its design in Section 4.3.

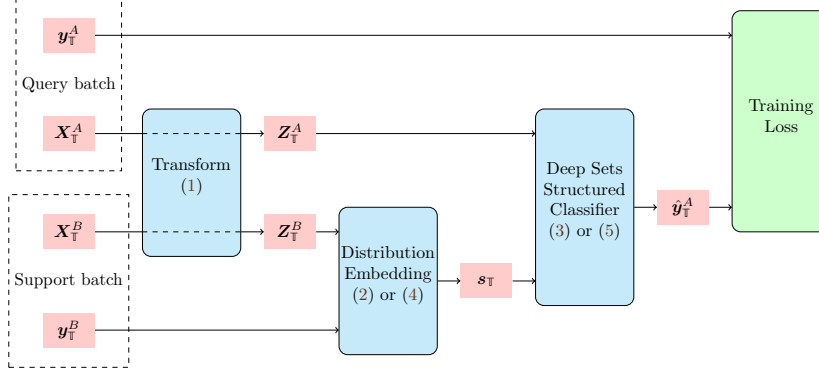


Figure 2: Block diagram of DEN for binary classification. During pre-training, for each gradient step we sample task $\mathbb{T} \in \{\mathbb{T}_1, \dots, \mathbb{T}_M\}$ and two batches of data from the task $(\mathbf{X}_{\mathbb{T}}^A, \mathbf{y}_{\mathbb{T}}^A)$ and $(\mathbf{X}_{\mathbb{T}}^B, \mathbf{y}_{\mathbb{T}}^B)$. During fine-tuning, we treat the support set as the support batch, using which to derive distribution embedding to make predictions on the query set, treated as the query batch.

4.1 Model Architecture for Binary Classification

To describe the model architecture of DEN for binary classification (illustrated in Figure 2), consider data (\mathbf{X}, \mathbf{y}) in a given task \mathbb{T} . DEN can be decomposed into three major blocks: transformation, embedding and classification. We will describe these blocks in this section.

Transforming covariates with task-dependent transformation block. We first transform the covariates via a transformation block, i.e.,

$$\mathbf{Z} = c(\mathbf{X}), \quad (1)$$

where $c: \mathbb{R}^d \rightarrow \mathbb{R}^d$ is applied to each row. Specifically, we use a piecewise linear function¹ (PLF) for each covariate, i.e., $c(\mathbf{x}) = (c^1(x^1), \dots, c^d(x^d))$. PLFs can be optionally constrained to be monotonic, which would serve as a form of regularization during training [14]. Note that the transformation block is task-dependent—its parameters need to be re-trained for each new task. The goal is that, after applying the corresponding transformation to each task, the relatedness across tasks increases. In contrast, existing meta-learning approaches usually do not have the transformation block and thus require the raw tasks to be related. This is conceptually similar to [29], where they consider the domain generalization problem and directly learn an invariant feature transformation by minimizing the dissimilarity across domains. To the contrary, we incorporate this block into a larger architecture and learn it in an end-to-end fashion.

One may instead consider other architectures than PLFs for the transformation block. We choose PLFs since they can implement compact one-dimensional non-linearities and can thus be fine-tuned with a small support set. Moreover, they are universal approximators: with enough keypoints, they can approximate any one-dimensional bounded continuous functions. In Section 5.3 we show that this PLF transformation is key to ensure good performance when training and target tasks have heterogeneous covariate spaces. PLFs cannot model interactions between covariates, which is a sacrifice we may have to make in light of the small support set. We study in Section 5.3 the trade-offs between the flexibility of PLF and the size of the support set.

Summarizing task statistics with task-independent distribution embedding block. The second block in DEN is to learn a vector that summarizes the task distribution. This is similar to Garnelo et al. [12]. Naïvely, one could learn a non-linear transformation ϕ which embeds (\mathbf{z}, \mathbf{y}) into a vector of smaller dimension. However, this would not work since the dimension of \mathbf{z} can vary across tasks. In contrast, we embed the

¹See Appendix A for the precise definition.

distribution $P(\mathbf{z}, y)$ of a given task into a vector using the transformed features \mathbf{Z} in the following way. For all $a, b \in [d]$, we derive a distribution embedding of $P(z^a, z^b, y)$ by

$$\mathbf{s}^{a,b} = \left(\overline{h(\mathbf{Z}_1^{a,b})}, \overline{h(\mathbf{Z}_2^{a,b})}, \overline{\mathbf{y}} \right), \quad (2)$$

where h is a vector-valued *trainable* function, and the average is taken with respect to the training batch during training and support set during inference, i.e.,

$$\overline{h(\mathbf{Z}_k^{a,b})} = \frac{\sum_{i=1}^n h(z_i^a, z_i^b) \mathbf{1}\{y_i = k\}}{\sum_{i=1}^n \mathbf{1}\{y_i = k\}},$$

and $\overline{\mathbf{y}} = \frac{1}{n} \sum_{i=1}^n y_i$. Note that n is about 50 in our setting, so the empirical average is close to the population counterpart. Intuitively, we decompose a variable-length feature vector \mathbf{z} into smaller pieces of fixed length 2, and use the h function to learn a pairwise embedding $\mathbf{s}^{a,b}$ for each pair of the 2 features a and b . This pairwise decomposition allows us to handle variable-length covariates. Note that the same function h is shared across all tasks, and it can be chosen as a few fully connected layers. The distribution embedding of $P(\mathbf{z}, y)$ is thus the set of embeddings of all pairs $\mathbf{s} = (\mathbf{s}^{a,b})_{a,b \in [d]}$.

Remark 4.1. The length 2 here is arbitrary. We can use pieces of length r for any $r \geq 1$, i.e., obtain an embedding $\mathbf{s}^{t_1, \dots, t_r}$ of $P(\mathbf{z}^{t_1, \dots, t_r}, y)$ for all $t_1, \dots, t_r \in [d]$. The larger r is the more expressive the model will be. We refer to r as the *dependency order*, and experiment with different values in Section 5.3.

Prediction with task-independent classification block. Given a query \mathbf{x} , we first transform it via $\mathbf{z} = c(\mathbf{x})$, and decompose the transformed features into sets of feature pairs. We then obtain the distribution embedding vector $\mathbf{s}^{a,b}$ of each pair in (2). Finally, we obtain the predicted logits using a Deep Sets architecture [50]:

$$q = \Phi(\mathbf{z}, \mathbf{s}) = \psi \left(\sum_{a,b \in [d]} \varphi([z^{a,b}, \mathbf{s}^{a,b}]) \right), \quad (3)$$

where φ is a vector-valued trainable function and ψ is a real-valued trainable function. Both φ and ψ are shared across tasks and can be chosen as fully connected layers. The Deep Sets architecture, which aggregates all possible pairs of covariates, is proven to be a universal approximator of set-input functions [50]. We note that one may use other set input architectures to construct the classification block, e.g., Set Transformer [22].

4.2 Model Architecture for Multiclass Classification

For multiclass classification tasks, we modify the distribution embedding and classification blocks. Specifically, we modify the distribution embedding in (2) as

$$\mathbf{s}^{a,b} = \frac{1}{n} \sum_{i=1}^n h([z_i^a, z_i^b, \mathbf{v}(y_i)]), \quad (4)$$

where $\mathbf{v} : \mathbb{N} \rightarrow \mathbb{R}^m$ is a vector-valued, trainable function that is shared across tasks— $\mathbf{v}(k)$ is hence a vector encoding of class k —and h is a vector-valued trainable function with input dimension $m + 2$.

For the classification block, we modify the idea of Matching Net [43], which is also similar to the modification adopted by Iwata and Kumagai [15]. This modification is suitable for tasks with different numbers of label classes. Let $\tilde{\Phi}$ be Φ in (3) without the last layer, i.e., $\tilde{\Phi}(\mathbf{z}, \mathbf{s}) = \sum_{a,b \in [d]} \varphi([z^{a,b}, \mathbf{s}^{a,b}])$ is the penultimate layer embedding of the query set example. We then obtain its class scores by

$$q_k = \frac{\sum_{i=1}^n \tilde{\Phi}(\mathbf{z}, \mathbf{s})^\top \tilde{\Phi}(\mathbf{z}_i, \mathbf{s}) \mathbf{1}\{y_i = k\}}{\sum_{i=1}^n \mathbf{1}\{y_i = k\}}. \quad (5)$$

Note that i in the above equation is the index of support set examples (n in total). The score q_k can thus be interpreted as the average dot-product of the penultimate layer embedding of the given query example with the penultimate embedding of the support set examples of class k . To obtain class probability, we apply a softmax on q_k 's.

4.3 Rationale for the Architectural Design

For further insights into the model architecture, consider the optimal Bayes classifier:

$$P(y = k \mid \mathbf{x}) = \frac{P(\mathbf{x} \mid y = k)P(y = k)}{\sum_{l=1}^L P(\mathbf{x} \mid y = l)P(y = l)}. \quad (6)$$

For a given task, if the conditional probability $P(\mathbf{x} \mid y = k)$ belongs to the same family of distributions for all $k \in [L]$, i.e., $\mathbf{x} \mid y = k \sim \phi(\mathbf{x}; \boldsymbol{\theta}_k)$, then the Bayes classifier can be constructed by estimating the parameters $\boldsymbol{\theta}_k$ and $P(y = k)$, and approximating the density ϕ as

$$P(y = k \mid \mathbf{x}) = \frac{\phi(\mathbf{x}; \hat{\boldsymbol{\theta}}_k) \hat{P}(y = k)}{\sum_{l=1}^L \phi(\mathbf{x}; \hat{\boldsymbol{\theta}}_l) \hat{P}(y = l)}. \quad (7)$$

If, additionally, $P(\mathbf{x} \mid y = k)$ belongs to the same family of distributions for all $k \in [L]$ and also all tasks, then the Bayes classifiers for all tasks should have the same functional form; only the parameters $\boldsymbol{\theta}_k$ and $P(y = k)$ differ by task. In this case, we can simply pool the data from all tasks together to estimate $\boldsymbol{\theta}_k$, $P(y = k)$ for each task, and the task-independent function ϕ .

However, the distribution family $\phi(\mathbf{x}; \boldsymbol{\theta}_k)$ may vary greatly across tasks. The task-dependent transformation block allows the transformed covariates to be in the same distribution family approximately. Then, we utilize the distribution embedding block to estimate the parameters $\boldsymbol{\theta}_k$ and $P(y = k)$. If all transformed covariates belong to the same distribution family, then the function form to estimate the parameters $\boldsymbol{\theta}_k$ and $P(y = k)$ should be identical for all tasks, which justifies our use of a *task-independent* distribution embedding block. Finally, we use the task-independent classification block to approximate the task-independent function ϕ and obtain a score for each label. The effectiveness of DEN depends crucially on the ability of the transformation block to align distribution families of covariates across tasks. We study in Section 5.3 the performance of DEN in relation to the flexibility of PLFs.

Finally, since the covariate dimension can vary across tasks, we decompose the covariate vector into sub-vectors of fixed length r and apply a Deep Sets architecture to these sub-vectors. In fact, Proposition 4.3 shows that if we consider the following family of densities, then the Bayes classifier must be of the form (3).

Definition 4.2. Let $\{f(\cdot; \boldsymbol{\theta}) : \mathbb{R}^r \rightarrow \mathbb{R}\}$ be a parametric family of functions (not necessarily densities). For any integer $d \geq r$, we say a function g on \mathbb{R}^d admits an *f-expansion* if it factorizes as $g(\mathbf{z}) = \prod_{t_{1:r} \in [d]^r} f(\mathbf{z}^{t_{1:r}}; \boldsymbol{\theta}^{t_{1:r}})$, where $\{\boldsymbol{\theta}^{t_{1:r}} \in \mathbb{R}^r\}$ is a set of parameters.

For instance, if $\mathbf{z} \mid y = 1 \sim \mathcal{N}_d(\boldsymbol{\mu}, \sigma^2 I_d)$, then the conditional density $p(\mathbf{z} \mid y = 1)$ is proportional to

$$\prod_{a=1}^d \frac{1}{\sigma} \exp\left(-\frac{(z^a - \mu^a)^2}{2\sigma^2}\right),$$

which admits an *f-expansion* with $r = 1$ and $\boldsymbol{\theta}^a = (\mu^a, \sigma)$.

Proposition 4.3. Let (\mathbf{z}, y) be a random vector in $\mathbb{R}^d \times [L]$ following some distribution P . Assume that the conditional density $p(\mathbf{z} \mid y = k)$ admits an *f-expansion* for some parametric family of functions $\{f(\cdot; \boldsymbol{\theta})\}$ on \mathbb{R}^r with parameters $\{\boldsymbol{\theta}_k^{t_{1:r}}\}$. Then there exist functions ψ and φ such that

$$P(y = k \mid \mathbf{z}) \propto \psi \left(\sum_{t_{1:r} \in [d]^r} \varphi(\mathbf{z}^{t_{1:r}}, \boldsymbol{\theta}_k^{t_{1:r}}, \pi_k) \right), \quad (8)$$

where $\mathbf{z}^{t_{1:r}} = (z^{t_1}, \dots, z^{t_r})$, $\pi_k = P(y = k)$, and ψ and φ only depend on f .

Table 1: Overview of training and evaluation.

Step	Input data	Transform	Embedding	Classification
Pre-training	Heterogeneous tasks $\{(\mathbf{x}_{\mathbb{T},i}, \mathbf{y}_{\mathbb{T},i})\}_{\mathbb{T},i}$	Trained	Trained	Trained
Fine-tuning	Support set $\{(\mathbf{x}_{\mathbb{S},i}, \mathbf{y}_{\mathbb{S},i})\}_i$	Trained $c_{\mathbb{S}}$	Fixed	Fixed
Evaluation	Query $\mathbf{x}_{\mathbb{S},q}$ and support set $\{(\mathbf{x}_{\mathbb{S},i}, \mathbf{y}_{\mathbb{S},i})\}_i$	Fixed $c_{\mathbb{S}}$	Fixed	Fixed

The proof is included in Appendix A. Note that our model (3) has exactly the same structure as the optimal Bayes classifier in (8) with $r = 2$ and \mathbf{s} representing the parameters $\{\boldsymbol{\theta}_k^{t_{1:r}}\}$ and marginal $\{\pi_k\}$. Proposition 4.3 shows that, under appropriate conditions, our model class is expressive enough to include the optimal Bayes classifier. This justifies our choice of the distribution embedding (2) and the Deep Sets structure (3). DEN will consequently performed well when learning across tasks whose conditional distributions of the PLF-transformed feature admits the same f -expansion. Heuristically, this means DEN is ideally applied to meta-learning settings in which features across tasks can be transformed to have a similar structure.

4.4 Training and Inference

Figure 2 shows a high level summary of our three-block model architecture. The overall training and evaluation procedure is summarized in Table 1. Note that all sets of r inputs use the same h and φ functions through parameter sharing, which reduces the size of the model. For DEN applied on tasks with d features, the feature transformation block has $\mathcal{O}(d)$ parameters. An embedding block with embedding order r , L layers and H hidden nodes per layer has $rH + H^2(L - 1)$ parameters. A classification block with L layers and H hidden nodes per layer for both the φ and ψ functions has $(r + 2)H + 2H^2L$ parameters. This DEN model is roughly of the same size as a $3L$ -layer deep H -node wide neural network. Empirically, we found that the computational complexity and resource requirement of DEN are similar to those of Vinyals et al. [43] and Iwata and Kumagai [15] given similar model sizes.

During pre-training, in each gradient step, we randomly sample a task $\mathbb{T} \in \{\mathbb{T}_t\}_{t=1}^M$ and two batches A and B from $(\mathbf{X}_{\mathbb{T}}, \mathbf{y}_{\mathbb{T}})$. These two batches are first transformed using PLFs in (1). We then use (2) or (4) to obtain a distribution embedding $\mathbf{s}_{\mathbb{T}}$, taking the average with respect to the examples in the support batch. Next, we use the distribution embedding to make predictions on the query batch using (3) or (5). Note that during training, $\mathbf{s}_{\mathbb{T}}$ is identical across examples within the same batch, but it could vary (even within the same task) across batches.

If PLFs can approximately transform the covariates so that they admit the same f -expansion, then the rest of the network is task-independent. Thus, after pre-training on $\{\mathbb{T}_t\}_{t=1}^M$, for each new task \mathbb{S} , we can fine-tune the transformation block (1), while keeping the weights of other blocks fixed. Because PLFs only have a small number of parameters, they can be trained on a small support set from the task \mathbb{S} .

During inference, we first use the learned PLFs in (1) to transform covariates in both the support set and the query set. We then utilize the learned distribution embedding block to obtain $\mathbf{s}_{\mathbb{S}}$, where the average in (2) and (4) is taken over the whole support set. Finally, the embedding $\mathbf{s}_{\mathbb{S}}$ and PLF-transformed query set covariates are used to classify query set examples using (3) or (5).

5 Numerical Studies

In Section 5.1, we use OpenML tabular datasets to demonstrate the performance of DEN on real-world tasks. DEN achieves the best performance among a number of baseline methods. We then introduce in Section 5.2 an approach to simulate binary classification tasks, which allows us to generate a huge amount of pre-training examples without the need of collecting real tasks. Surprisingly, DEN (and several other methods) trained on simulated data can sometimes outperform those trained on real data. In Section 5.3, we examine the performance of DEN in relation to different architecture and hyper-parameter choices. The findings are: (a)

Table 2: Average test AUC (standard error) and the percent of times that each method achieves the best performance on 20 OpenML datasets \times 20 repeats.

Method	Average Test AUC (%)	% Best
Matching Net	50.11 (0.04)	0.00%
Proto Net	71.11 (0.72)	27.50%
PMN	56.11 (0.65)	0.75%
Relation Net	51.65 (0.28)	0.25%
CNP	58.01 (0.69)	7.00%
Iwata and Kumagai [15]	70.35 (0.70)	26.75%
MAML	60.64 (0.82)	7.00%
T-Net	52.22 (0.41)	0.5%
DEN	70.12 (0.83)	30.25%

PLF and fine-tuning are crucial when the training and test tasks are unrelated (e.g., when training tasks are simulated), whereas their effect is insignificant when the tasks are similar, and (b) the performance of DEN is relatively stable for small values of the dependency order r in Remark 4.1.

Baseline methods for comparison with DEN include Matching Net [43], Proto Net [40], TADAM [33], PMN [45], Relation Net [41], CNP [12], MAML [10], BMAML [11], T-Net [23] and Iwata and Kumagai [15]. Hyperparameters of all methods are chosen based on cross-validation on training tasks. Hyperparameters, model structures and implementation details are summarized in Appendix B. Note that we set the dependency order $r = 2$ if it is not stated explicitly. For MAML, BMAML and T-net, we fine-tune the last layer of the base model for 5 epochs on the support set. For the rest of the methods, we train them with episodic training² [43]. For methods that do not readily handle variable length inputs, we randomly repeat features to make all tasks have the same length of inputs.

5.1 Results on OpenML Classification Tasks

5.1.1 Binary classification

We compare DEN with baseline methods on 20 OpenML binary classification datasets [42] following the setup in Iwata and Kumagai [15] (see a list of datasets in Appendix C). These datasets have examples ranging from 200 to 1,000,000 and features ranging from 2 to 25.

We pre-train DEN and baseline methods on the OpenML datasets in the leave-one-dataset-out fashion. That is, for each of the 20 OpenML datasets chosen as a target task, we pretrain the models on the remaining 19 datasets. For the target task, we randomly select 50 examples to form the support set, and use the rest of the dataset as the query set. We repeat the whole procedure 20 times, and report the average AUC and the percentage that each method achieves the best performance in Table 2 based on 20 test sets \times 20 repeats. DEN has average AUC comparable with the best methods, and the highest frequency that it achieves the best AUC. As a comparison, directly training task-specific linear models on the support set of each task gives an average test AUC of 57.15%. Directly training an 1 hidden layer, 8 hidden nodes neural network on the support set gives an average test AUC of 54.58%. With 2 hidden layers, AUC drops to 53.00% and with 3 hidden layers, 49.74%. DEN significantly outperforms those methods. These results demonstrate the effect of over-fitting for classical methods on small data, and the benefit of DEN over classical methods on those small-data problems. In Section 5.2, we will further describe an approach to generate binary classification training tasks through controlled simulation. DEN trained on simulated tasks, surprisingly, outperforms DEN trained on real tasks, and, in fact, achieves the best performance among all competing methods.

²Code is available at https://github.com/google-research/google-research/distribution_embedding_networks.

Table 3: Average test accuracy (standard error) and the percent of times that each method achieves the best performance on 8 OpenML datasets \times 20 repeats.

Method	Average Test Accuracy (%)	% Best
Direct NN	45.68 (1.56)	13.6%
Matching Net	46.36 (1.55)	13.8%
Proto Net	33.68 (1.80)	4.9%
PMN	24.77 (0.63)	0.0%
Relation Net	33.49 (1.82)	4.9%
CNP	18.77 (1.53)	1.1%
Iwata and Kumagai [15]	24.93 (0.62)	0.0%
DEN	48.60 (1.51)	61.6%

5.1.2 Multiclass classification

In addition to binary classification tasks, we also compare DEN with baseline methods on 8 OpenML multi-class classification datasets. These datasets have examples ranging from 400 to 1,000,000, features ranging from 5 to 23, and number of classes ranging from 3 to 7. We train DEN and baseline methods on the OpenML datasets in the same leave-one-dataset-out fashion as in the binary classification. Results are summarized in Table 3. DEN achieved the best performance, followed by Matching Net. We also compare against directly training a neural network (NN) on the support set, which achieved decent accuracy. But DEN remains the best methods in majority (61.6%) of cases.

5.2 Generate Training Tasks through Controlled Simulation

In this section, we describe an approach to generate binary classification pre-training tasks based on model aggregation. Comparing to pre-training meta-learning models on related real-world datasets, which could be expensive to collect, this synthetic approach can easily give us a huge amount of pre-training examples. We will show that meta-learning methods trained with simulated data can, surprisingly, sometimes outperform those trained with real data.

Specifically, we first take seven image classification datasets: CIFAR-10, CIFAR-100 [18], MNIST [19], Fashion MNIST [47], EMNIST [4], Kuzushiji MNIST [KMNIST; 3] and SVHN [32]. On each dataset, we pick nine equally spaced cutoffs and binarize the labels based on whether the class id is below the cutoff. This gives nine binary classification tasks for each dataset with positive label proportion in $\{0.1, 0.2, \dots, 0.9\}$.

To generate covariates for each task, we build 50 convolution image classifiers of various model complexities (details in Appendix B) on each of the 63 tasks to predict the binary label. We take classification scores on the test set as covariates. With these covariates and associated labels, we construct $7 \times 9 = 63$ binary classification tasks $\{\mathbb{T}_1, \dots, \mathbb{T}_{63}\}$. Essentially, they are model aggregation tasks since we are combining 50 classifiers to make a prediction. Note that the accuracy of those image classifiers ranges from below 0.6 to over 0.99, giving rise to covariates ranging widely in their signal-to-noise ratios.

Finally, to augment training data, we apply covariate sampling during pre-training. In each pre-training step, we first randomly sample an integer $C \in \{1, \dots, 50\}$ and a task from the 63 aggregation tasks $\{\mathbb{T}_1, \dots, \mathbb{T}_{63}\}$ described above. Then, among the 50 convolution image classifiers we built, we randomly pick C of them and use their classification scores as covariates to construct a *sub-task*. Finally, DEN takes labeled examples from this sub-task and uses them for training in this step. We shall emphasize that although training tasks are built based on image classification datasets, we do *not* use raw pixel values as covariates in pre-training.

Table 4: Average test AUC (standard error) and the percent of times that each method achieves the best performance on 20 OpenML datasets \times 20 repeats. The models are pre-trained on simulated data. We also report the improvement in average test AUC compared to pre-training on OpenML data.

Method	Average Test AUC (%)	% Best	Improv. in Test AUC (%)
Matching Net	53.88 (0.46)	0.00%	3.77 (0.46)
Proto Net	71.12 (0.65)	28.00%	0.01 (0.97)
PMN	59.04 (0.68)	1.25%	2.93 (0.94)
Relation Net	57.97 (0.59)	0.00%	6.32 (0.65)
CNP	60.95 (0.69)	2.50%	2.94 (0.98)
Iwata and Kumagai [15]	66.01 (0.74)	11.50%	-4.34 (1.02)
MAML	61.16 (0.66)	2.75%	0.52 (1.05)
T-Net	53.35 (0.46)	0.25%	1.13 (0.62)
DEN	74.13 (0.68)	53.75%	4.01 (1.07)

OpenML binary classification with simulated training tasks. To illustrate the effectiveness of our data simulation approach, we use the models pre-trained on these data and evaluate them on the same 20 OpenML binary classification tasks in Section 5.1 after fine-tuning. Interestingly, as shown in Table 4, for 5 out of the 9 methods considered, pre-training on the simulated data gives us statistically significantly better test AUC. This suggests that the proposed approach to generate training tasks is not only convenient but also effective. Moreover, DEN pre-trained on the simulated data outperforms all methods (either pre-trained on the simulated data or OpenML data) significantly.

5.3 Effect of Dependence Order, PLF, and Fine-tuning

We continue our examination of DEN with pre-training on simulated data. In addition to comparing DEN with competing methods, we also study the performance of DEN in relation to its dependence order r , and the use of PLF and fine-tuning. For DEN, we explore three options: 1) fine-tune the PLF layer for 10 epochs, 2) take the PLF layer directly from the last pre-training epoch without fine-tuning, or 3) do not include a PLF layer in DEN and hence no fine-tuning at all.

5.3.1 Tasks with Heterogeneous Covariate Spaces

We study and demonstrate the importance of PLF when the training and test tasks are heterogeneous. Specifically, we use all 63 simulated tasks described in Section 5.2 for pre-training, and test the performance on two real datasets: Nomao and Puzzles. We give a short description of each dataset in Section C.

For each dataset, we repeat the whole procedure 20 times and report the average AUC and standard error in Table 5. It is clear that DEN outperforms other baseline methods significantly. More importantly, the results also show that fine-tuning and PLF greatly improve the performance of DEN. Since DEN is pre-trained on simulated tasks which are completely unrelated to the target task, this improvement demonstrates the importance of fine-tuning and PLF when the training and target tasks are heterogeneous.

We also examine the effect of the size of the support set on the flexibility of the covariate transformation block. Figure 3 shows that with enough support set examples (e.g., Puzzles task), having more PLF keypoints benefits the test performance due to the improved ability of task-adaptation. However, if the support set is small (e.g., Nomao task), having a flexible covariate transformation block could even be marginally harmful.

Finally, we conduct an ablation study to examine the effect of dependency order in Remark 4.1 on the test AUC on the Nomao dataset. In particular, we examine DEN with $r \in [8]$. The results in Table 6 show that when $r \leq 5$, the test AUC is relatively stable, with the best performance achieved at $r = 2$; whereas the test AUC is much worse and unstable for larger r .

Table 5: Average test AUC (standard error) on Nomao and Puzzles data.

Method	Nomao	Puzzles
Matching Net	73.18 (2.23)	62.65 (1.45)
Proto Net	80.56 (0.56)	73.77 (0.37)
TADAM	82.42 (0.35)	74.86 (0.25)
PMN	77.00 (3.13)	57.69 (1.53)
Relation Net	52.32 (1.61)	63.73 (1.79)
CNP	91.40 (0.36)	53.20 (0.12)
Iwata and Kumagai [15]	66.85 (3.23)	61.32 (0.52)
MAML	78.92 (2.22)	54.92 (0.54)
BMAML	47.20 (3.40)	53.49 (1.88)
T-Net	61.42 (3.44)	54.55 (1.78)
DEN w/o PLF w/o FT	59.01 (1.04)	68.87 (0.38)
DEN w/o FT	94.42 (0.16)	70.74 (0.62)
DEN	95.21 (0.10)	78.11 (0.53)

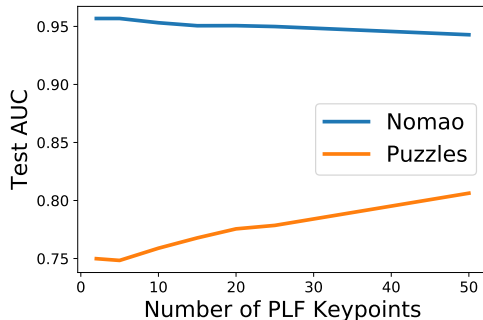


Figure 3: Average test AUC versus the number of PLF keypoints on Nomao and Puzzles data.

5.3.2 Tasks with Homogeneous Covariate Spaces

We study the performance of DEN in the case when the training and target tasks are homogeneous. To ensure the task homogeneity, we use the model aggregation tasks described in Section 5.2 for both training and evaluation. Specifically, we use the $5 \times 9 = 45$ tasks described in Section 5.2 derived from CIFAR-10, CIFAR-100, MNIST, Fashion MNIST and EMNIST to train DEN and other meta-learning methods. We then pick four test tasks from SVHN and KMNIST of different difficulties, where the average AUCs over 50 classifiers are 68.28%, 78.11%, 91.51%, and 87.58%, respectively. Note that the training and test tasks are totally separated, but they likely follow similar distributions since the covariates for training and tests are all classifier scores.

For each test task, we randomly select 100 sets of C classifiers among the 50 candidate classifiers, resulting in 100 aggregation sub-tasks. For each aggregation sub-task, we form a support set with 50 labeled examples and a disjoint query set with 8000 examples. We repeat the entire training and fine-tuning process for 5 times, and report the average AUC and its standard error.

Table 7 shows the result of aggregating an ensemble of $C = 25$ classifiers. Table 8 shows the result where the number of classifiers C to be aggregated is sampled uniformly from $[13, 25]$ and could vary across sub-tasks (100 aggregation sub-tasks \times 5 repeats). To allow baseline methods to take varying number of covariates, we randomly duplicate some of the C classifiers so that all inputs have 25 covariates.

Table 6: Average test AUC (standard error) of DEN on Nomao data with different dependency order.

$r = 1$	$r = 2$	$r = 3$	$r = 4$
94.38 (0.46)	95.21 (0.10)	93.80 (0.25)	92.61 (0.55)
$r = 5$	$r = 6$	$r = 7$	$r = 8$
93.16 (0.45)	91.22 (0.74)	88.95 (2.02)	89.15 (1.34)

Table 7: Average test AUC (standard error) when aggregating 25 classifiers.

Method	Test AUC (%)			
	Task 1	Task 2	Task 3	Task 4
Matching Net	70.01 (0.40)	82.13 (0.05)	95.29 (0.06)	93.82 (0.08)
Proto Net	90.95 (0.05)	89.84 (0.03)	98.07 (0.01)	97.40 (0.02)
TADAM	90.98 (0.05)	89.90 (0.03)	98.14 (0.01)	97.57 (0.02)
PMN	86.78 (0.10)	88.69 (0.03)	97.46 (0.02)	96.22 (0.05)
Relation Net	85.39 (0.15)	88.70 (0.02)	97.25 (0.02)	95.55 (0.08)
CNP	86.53 (0.09)	88.80 (0.02)	97.50 (0.02)	96.22 (0.05)
Iwata and Kumagai [15]	89.33 (0.05)	89.17 (0.02)	97.93 (0.01)	97.73 (0.02)
MAML	86.10 (0.11)	88.78 (0.03)	97.48 (0.02)	96.13 (0.06)
BMAML	71.38 (0.84)	85.96 (0.21)	97.04 (0.08)	95.39 (0.18)
T-Net	86.23 (0.10)	88.76 (0.03)	97.47 (0.02)	96.11 (0.06)
DEN w/o PLF w/o Fine-Tuning	91.53 (0.03)	90.18 (0.02)	98.03 (0.01)	98.37 (0.01)
DEN w/o Fine-Tuning	91.76 (0.03)	90.20 (0.02)	98.18 (0.01)	98.41 (0.01)
DEN	91.80 (0.03)	89.77 (0.02)	97.38 (0.01)	97.23 (0.01)

We observe that DEN significantly outperforms other methods in all tasks, and that DEN without PLF and/or without fine-tuning is statistically no worse than DEN with fine-tuning on the PLF layer. This suggests that fine-tuning the PLF layer is not necessary when the data distribution is similar among tasks.

6 Conclusion

In this work, we introduce a novel meta-learning method that can be applied to settings where both the distribution and number of covariates vary across tasks. This allows us to train the model on a wider range of training tasks and then adapt it to a variety of target tasks. Most other meta-learning techniques do not readily handle such settings. In numerical studies, we demonstrate that the proposed method outperforms a number of meta-learning baselines.

The proposed model consists of three flexible building blocks. Each block can be replaced by more advanced structures to further improve its performance. DEN can also be combined with optimization based meta-learning methods, e.g., MAML. A limitation of DEN is that it requires calculating the embedding for d^r different combinations of covariates, which is infeasible for high-dimensional tasks. A potential solution is to use a random subset of these combinations. We leave the exploration of these options for future work.

Table 8: Average test AUC (standard error) when aggregating variable number of classifiers.

Method	Test AUC (%)			
	Task 1	Task 2	Task 3	Task 4
Matching Net	75.16 (0.37)	81.12 (0.08)	95.86 (0.04)	93.61 (0.08)
Proto Net	90.02 (0.11)	89.65 (0.04)	97.94 (0.02)	97.57 (0.02)
TADAM	90.20 (0.10)	89.74 (0.04)	98.04 (0.01)	97.84 (0.01)
PMN	85.68 (0.24)	88.59 (0.04)	97.30 (0.03)	95.83 (0.08)
Relation Net	80.85 (0.65)	88.53 (0.04)	97.11 (0.04)	95.03 (0.12)
CNP	84.97 (0.28)	88.71 (0.04)	97.31 (0.04)	95.96 (0.07)
Iwata and Kumagai [15]	89.26 (0.16)	89.05 (0.03)	97.82 (0.02)	97.75 (0.02)
MAML	85.39 (0.23)	88.53 (0.04)	97.32 (0.04)	95.86 (0.08)
BMAML	59.57 (1.07)	85.40 (0.24)	96.73 (0.10)	94.53 (0.23)
T-Net	85.51 (0.22)	88.55 (0.04)	97.35 (0.03)	95.94 (0.07)
DEN w/o PLF w/o Fine-Tuning	91.06 (0.09)	89.92 (0.03)	98.09 (0.01)	98.24 (0.01)
DEN w/o Fine-Tuning	91.17 (0.09)	89.95 (0.03)	97.95 (0.01)	98.10 (0.01)
DEN	91.29 (0.03)	89.83 (0.02)	97.60 (0.03)	97.47 (0.01)

References

- [1] H. Altae-Tran, B. Ramsundar, A. S. Pappu, and V. Pande. Low data drug discovery with one-shot learning. *ACS Central Science*, 3(4), 2017.
- [2] L. Bertinetto, J. F. Henriques, J. Valmadre, P. H. S. Torr, and A. Vedaldi. Learning feed-forward one-shot learners. In *NIPS*, 2016.
- [3] T. Clanuwat, M. Bober-Irizar, A. Kitamoto, A. Lamb, K. Yamamoto, and D. Ha. Deep learning for classical Japanese literature. *NeurIPS Workshop on Machine Learning for Creativity and Design*, 2018.
- [4] G. Cohen, S. Afshar, J. Tapson, and A. V. Schaik. EMNIST: Extending MNIST to handwritten letters. In *IJCNN*, 2017.
- [5] W. Dai, Y. Chen, G. Xue, Q. Yang, and Y. Yu. Translated learning: Transfer learning across different feature spaces. In *NIPS*, 2008.
- [6] O. Day and T. M. Khoshgoftaar. A survey on heterogeneous transfer learning. *Journal of Big Data*, 4, 2017.
- [7] T. Deleu and Y. Bengio. The effects of negative adaptation in model-agnostic meta-learning. *arXiv preprint*, 2018.
- [8] L. Duan, D. Xu, and I. W. Tsang. Learning with augmented features for heterogeneous domain adaptation. In *ICML*, 2012.
- [9] H. Edwards and A. Storkey. Towards a neural statistician. In *ICLR*, 2017.
- [10] C. Finn, P. Abbeel, and S. Levine. Model-agnostic meta-learning for fast adaptation of deep networks. In *ICML*, 2017.
- [11] C. Finn, K. Xu, and S. Levine. Probabilistic model-agnostic meta-learning. In *NeurIPS*, 2018.

- [12] M. Garnelo, D. Rosenbaum, C. Maddison, T. Ramalho, D. Saxton, M. Shanahan, Y. W. Teh, D. Rezende, and S. M. A. Eslami. Conditional neural processes. In *ICML*, 2018.
- [13] E. Grant, C. Finn, S. Levine, T. Darrell, and T. Griffiths. Recasting gradient-based meta-learning as hierarchical Bayes. In *ICLR*, 2018.
- [14] M. Gupta, A. Cotter, J. Pfeifer, K. Voevodski, K. Canini, A. Mangylov, W. Moczydlowski, and A. van Esbroeck. Monotonic calibrated interpolated look-up tables. *Journal of Machine Learning Research*, 17(109), 2016.
- [15] T. Iwata and A. Kumagai. Meta-learning from tasks with heterogeneous attribute spaces. In *NeurIPS*, 2020.
- [16] L. Kaiser, O. Nachum, A. Roy, and S. Bengio. Learning to remember rare events. In *ICLR*, 2017.
- [17] G. Koch, R. Zemel, and R. Salakhutdinov. Siamese neural networks for one-shot image recognition. In *ICML*, 2015.
- [18] A. Krizhevsky. Learning multiple layers of features from tiny images. Technical report, University of Toronto, 2009.
- [19] Y. LeCun, C. Cortes, and C. Burges. MNIST handwritten digit database. *ATT Labs [Online]*. Available: <http://yann.lecun.com/exdb/mnist>, 2010.
- [20] H. Lee, E. Hyung, and S. J. Hwang. Rapid neural architecture search by learning to generate graphs from datasets. In *ICLR*, 2021.
- [21] H. B. Lee, H. Lee, D. Na, S. Kim, M. Park, E. Yang, and S. J. Hwang. Learning to balance: Bayesian meta-learning for imbalanced and out-of-distribution tasks. In *ICLR*, 2020.
- [22] J. Lee, Y. Lee, J. Kim, A. Kosiorek, S. Choi, and Y. W. Teh. Set Transformer: A framework for attention-based permutation-invariant neural networks. In *ICML*, 2019.
- [23] Y. Lee and S. Choi. Gradient-based meta-learning with learned layerwise metric and subspace. In *ICML*, 2018.
- [24] H. Li, S. J. Pan, S. Wang, and A. C. Kot. Domain generalization with adversarial feature learning. In *CVPR*, 2018.
- [25] W. Li, L. Duan, D. Xu, and I. W. Tsang. Learning with augmented features for supervised and semi-supervised heterogeneous domain adaptation. *IEEE Transactions on Pattern Analysis and Machine Intelligence*, 36(6), 2014.
- [26] Y. Li, X. Tian, M. Gong, Y. Liu, T. Liu, K. Zhang, and D. Tao. Deep domain generalization via conditional invariant adversarial networks. In *ECCV*, 2018.
- [27] Y. Liu, J. Lee, M. Park, S. Kim, E. Yang, S. Hwang, and Y. Yang. Learning to propagate labels: Transductive propagation network for few-shot learning. In *ICLR*, 2019.
- [28] N. Mishra, M. Rohaninejad, X. Chen, and P. Abbeel. A simple neural attentive meta-learner. In *ICLR*, 2018.
- [29] K. Muandet, D. Balduzzi, and B. Schölkopf. Domain generalization via invariant feature representation. In *ICML*, 2013.
- [30] T. Munkhdalai and H. Yu. Meta networks. In *ICML*, 2017.
- [31] T. Munkhdalai, X. Yuan, S. Mehri, and A. Trischler. Rapid adaptation with conditionally shifted neurons. In *ICML*, 2018.

- [32] Y. Netzer, T. Wang, A. Coates, A. Bissacco, B. Wu, and A. Y. Ng. Reading digits in natural images with unsupervised feature learning. *NIPS Workshop on Deep Learning and Unsupervised Feature Learning*, 2011.
- [33] B. N. Oreshkin, P. R. López, and A. Lacoste. TADAM: task dependent adaptive metric for improved few-shot learning. In *NeurIPS*, 2018.
- [34] S. Ravi and H. Larochelle. Optimization as a model for few-shot learning. In *ICLR*, 2017.
- [35] A. A. Rusu, D. Rao, J. Sygnowski, O. Vinyals, R. Pascanu, S. Osindero, and R. Hadsell. Meta-learning with latent embedding optimization. In *ICLR*, 2019.
- [36] A. Santoro, S. Bartunov, M. Botvinick, D. Wierstra, and T. Lillicrap. Meta-learning with memory-augmented neural networks. In *ICML*, 2016.
- [37] V. G. Satorras and J. B. Estrach. Few-shot learning with graph neural networks. In *ICLR*, 2018.
- [38] S. Shankar, V. Piratla, S. Chakrabarti, S. Chaudhuri, P. Jyothi, and S. Sarawagi. Generalizing across domains via cross-gradient training. In *ICLR*, 2018.
- [39] J. Shen, Y. Qu, W. Zhang, and Y. Yu. Wasserstein distance guided representation learning for domain adaptation. In *AAAI*, 2018.
- [40] J. Snell, K. Swersky, and R. S. Zemel. Prototypical networks for few-shot learning. In *NIPS*, 2017.
- [41] F. Sung, Y. Yang, L. Zhang, T. Xiang, P. H. S. Torr, and T. M. Hospedales. Learning to compare: Relation network for few-shot learning. In *CVPR*, 2018.
- [42] J. Vanschoren, J. N. van Rijn, B. Bischl, and L. Torgo. OpenML: Networked science in machine learning. *SIGKDD Explorations*, 15(2), 2013.
- [43] O. Vinyals, C. Blundell, T. Lillicrap, K. Kavukcuoglu, and D. Wierstra. Matching networks for one shot learning. In *NIPS*, 2016.
- [44] J. Wang, C. Lan, C. Liu, Y. Ouyang, and T. Qin. Generalizing to unseen domains: A survey on domain generalization. In *IJCAI*, 2021.
- [45] Y. Wang, R. B. Girshick, M. Hebert, and B. Hariharan. Low-shot learning from imaginary data. In *CVPR*, 2018.
- [46] Y. Wang, Q. Yao, J. T. Kwok, and L. M. Ni. Generalizing from a few examples: A survey on few-shot learning. *ACM Computing Surveys*, 53(3), 2020.
- [47] H. Xiao, K. Rasul, and R. Vollgraf. Fashion-MNIST: a novel image dataset for benchmarking machine learning algorithms. *ArXiv preprint*, 2017.
- [48] Y. Yan, W. Li, M. K. P. Ng, M. Tan, H. Wu, H. Min, and Q. Wu. Learning discriminative correlation subspace for heterogeneous domain adaptation. In *IJCAI*, 2017.
- [49] Q. Yang, Y. Chen, G.-R. Xue, W. Dai, and Y. Yu. Heterogeneous transfer learning for image clustering via the social web. In *Joint Conference of ACL and IJCNLP*, 2009.
- [50] M. Zaheer, S. Kottur, S. Ravanbakhsh, B. Póczos, R. Salakhutdinov, and A. J. Smola. Deep sets. In *NIPS*, 2017.
- [51] J. T. Zhou, I. W. Tsang, S. J. Pan, and M. Tan. Multi-class heterogeneous domain adaptation. *Journal of Machine Learning Research*, 20, 2019.
- [52] K. Zhou, Z. Liu, Y. Qiao, T. Xiang, and C. C. Loy. Domain generalization: A survey. *arXiv preprint*, 2021.

A Details and Proofs

Piecewise linear function. The piecewise linear function (PLF) $c_{\mathbb{T}}^j : \mathbb{R} \rightarrow \mathbb{R}$ for each covariate j and task \mathbb{T} is defined by

$$c_{\mathbb{T}}^j(x; \mathbf{k}_{\mathbb{T}}^j, \boldsymbol{\alpha}_{\mathbb{T}}^j) := \sum_{l=1}^{K-1} \mathbb{1}\left(k_{\mathbb{T},l}^j \leq x \leq k_{\mathbb{T},l+1}^j\right) \ell_{\mathbb{T},l}^j(x), \quad (9)$$

$$\ell_{\mathbb{T},l}^j(x) := \alpha_{\mathbb{T},l}^j + \frac{x - k_{\mathbb{T},l}^j}{k_{\mathbb{T},l+1}^j - k_{\mathbb{T},l}^j} \left(\alpha_{\mathbb{T},l+1}^j - \alpha_{\mathbb{T},l}^j\right),$$

where $\mathbf{k}_{\mathbb{T}}^j := [k_{\mathbb{T},1}^j, \dots, k_{\mathbb{T},K}^j] \in \mathbb{R}^K$, $k_{\mathbb{T},1}^j < k_{\mathbb{T},2}^j < \dots < k_{\mathbb{T},K}^j$, is the vector of *predetermined* keypoints that spans the domain of $x_{\mathbb{T}}^j$, and $\boldsymbol{\alpha}_{\mathbb{T}}^j := [\alpha_{\mathbb{T},1}^j, \dots, \alpha_{\mathbb{T},K}^j] \in \mathbb{R}^K$ is the parameter vector, characterizing the output at each keypoint.

Proof of Proposition 4.3. By the Bayes' rule, for each $k \in [L]$,

$$P(y = k | \mathbf{z}) \propto p(\mathbf{z} | y = k) p(y = k) = \pi_k \prod_{t_{1:r} \in [d]^r} f(\mathbf{z}^{t_{1:r}}; \boldsymbol{\theta}_k^{t_{1:r}}).$$

Define the function φ by

$$\varphi(\mathbf{z}^{t_{1:r}}, \boldsymbol{\theta}_k^{t_{1:r}}, \pi_k) = \log f(\mathbf{z}^{t_{1:r}}; \boldsymbol{\theta}_k^{t_{1:r}}) + \frac{1}{d^r} \log \pi_k,$$

and define $\psi(x) = e^x$. Then it is clear that

$$P(y = k | \mathbf{z}) \propto \psi \left(\sum_{t_{1:r} \in [d]^r} \varphi(\mathbf{z}^{t_{1:r}}, \boldsymbol{\theta}_k^{t_{1:r}}, \pi_k) \right).$$

□

B Model Structures and Hyperparameters

In this section, we report model structures and hyperparameters of all models we have considered in our experiments.

To generate training tasks, the 50 convolutional image classifiers all have the structure $\text{Conv}(f, k) \rightarrow \text{MaxPool}(p) \rightarrow \text{Conv}(f, k) \rightarrow \text{MaxPool}(p) \rightarrow \dots \rightarrow \text{Conv}(f, k) \rightarrow \text{Dense}(u) \rightarrow \text{Dense}(u) \rightarrow \dots \rightarrow \text{Dense}(1)$, where the number of dense layers $d \in [1, 4]$, number of convoluted layers $c \in [0, 3]$, filters and units $f, u \in [2, 511]$, kernel and pool sizes $k, p \in [2, 5]$, and training epochs $e \in [1, 24]$ are uniformly sampled.

We use 5-fold cross-validation on 5×9 tasks of aggregating 25 classifiers derived from CIFAR-10, CIFAR-100, MNIST, Fashion MNIST and EMNIST to tune the hyperparameters. In each fold, we trained the model on all but one training datasets and evaluated it on the remaining one³, feeding with 50 supporting examples; we then selected the model with the highest AUC scores averaged over 5 folds.

For DEN, Matching Net, Proto Net, TADAM, PMN, Relation Net and CNP, we trained each of them for 200 epochs using Adam optimizer with batch size 256 and the TensorFlow default learning rate, 0.001. We did not apply fine-tuning on those methods.

For MAML, BMAML, T-Net, we first train a base model (either a DNN or a T-Net) for 1000 steps. In each step, we randomly sample 10 sub-tasks of batch size 256 from 36 training tasks. After these 1000 steps,

³For example, in one of the five folds, we trained the models on 4×9 tasks derived from CIFAR-10, CIFAR-100, MNIST and Fashion MNIST datasets, and evaluated the model on the 9 tasks derived from the EMNIST dataset

we fine-tuned the last layer of the trained DNN or T-net on a support set of size 50 of each validation task for 6 epochs, then evaluated it on the remaining examples of this validation task.

Note that, during hyperparameter tuning, the maximum number of ReLU-activated dense layers we have tried is 12 and the maximum number of units we have tried is 128 for all models. The proposed Joint DEN and Conditional DEN tend to prefer larger models than the rest ones. Based on cross-validation, we arrived at the following model architectures.

Matching Net. For Matching Net, we used the formulation with the attention kernel. The full context embedding is examined with the PMN model. Both the f and g embedding functions were 1-hidden-layer, 64-unit DNNs with ReLU activation, which output 64-dimensional embeddings.

Proto Net. For Proto Net, the embedding model f_ϕ was a 1-hidden-layer, 32-unit DNN with ReLU activation, which outputs 32-dimensional embeddings. The distance metric is taken as the Euclidean norm.

TADAM. For TADAM, the task representation model f_ϕ was a 1-hidden-layer, 32-unit DNN with ReLU activation, which outputs 32-dimensional embeddings. The γ and β models were each a 1-hidden-layer, 32-unit DNN with ReLU activation, which each outputs 64 values. The post multipliers γ_0 and β_0 were ridge regularized with weight 0.01. We modified the weights of the task representation model based on γ and β as in the FILM conditioning layer to get the class representation model. The similarity metric was taken as the Euclidean norm with metric scaling.

PMN. For PMN, the embedding model was a 3-hidden-layer, 32-unit ReLU activated DNN with 32-dimensional output. The bidirectional LSTM and attention LSTM each has units. To build the attention LSTM, we use $K = 8$ ‘‘Process’’ blocks. The distance metric was Euclidean norm.

Relation Net. For Relation Net, the f_ψ embedding model was a 1-hidden-layer, 32-unit DNN with ReLU activation and 32-dimensional output. The relation model g_ϕ was a 2-hidden-layer, 16-unit DNN with ReLU activation.

CNP. For CNP, the embedding model h_θ was a 1-hidden-layer, 64-unit DNN with ReLU activation and 64 dimensional output. The commutative operation was taken to be average operation. The prediction model g_θ was a 2-hidden-layer, 8-unit DNN with ReLU activation.

MAML. For MAML, the base model is a 4-hidden-layer, 64 unit ReLU activated DNN model. The MAML learning rates are $\alpha = 0.01$ for the inner loop and $\beta = 0.005$ for the outer loop.

BMAML. For BMAML, the base model is a 4-hidden-layer, 64 unit ReLU activated DNN model. The BMAML inner loop learning rate is $\alpha = 0.01$. The step size parameters γ_p and γ_q were initialized as a constant vector with value 0.00005, and the variance parameters v_q and σ_θ^2 were initialized as diagonal matrices with value 0.0001.

T-Net. For T-Net, the base model is a T-Net with 4 32-unit W layers and 4 32-unit T layers (the last, i.e., output, T layer has 1-unit). The activation function σ is ReLU. The learning rates were $\alpha = \beta = 0.01$.

DEN. For DEN, we used PLFs with 10 calibration keypoints, uniformly distributed in the input domain. The distribution embedding model was a 3-hidden-layer, 16-unit ReLU activated DNN with 16 dimensional output. We took the mean embedding over the batch to get the distribution embedding. The Deep Sets classification model is a 3-hidden-layer, 64-unit ReLU activated DNN, followed by mean pooling and another 4-hidden-layer, 64-unit ReLU activated DNN.

Data Name	OpenML ID	# Fine-Tune	# Test	# Features
BNG Australian	1205	50	999950	14
BNG breast-w	251	50	39316	9
BNG credit-g	40514	50	999950	20
BNG heart-statlog	251	50	999950	13
Hyperplane 10 1E-3	152	50	999950	10
SEA 50	161	50	999950	3
ada prior	1037	50	4512	14
adult	1590	50	48792	14
churn	40701	50	4950	20
cleve	40710	50	253	13
cpu act	761	50	8142	21
default-of-credit-card-clients	42477	50	29950	23
disclosure x tampered	795	50	612	3
fri c2 250 25	794	50	200	25
fri c3 250 10	793	50	200	10
irish	451	50	450	5
phoneme	1489	50	5354	5
strikes	770	50	575	6
sylvine	41146	50	5074	20
wholesale-customers	41146	50	390	8

Table 9: List of statistics of 20 OpenML binary classification datasets used in numerical studies.

C Description of Real Datasets

With Nomao data, we use fax trigram similarity score, street number trigram similarity score, phone trigram similarity score, clean name trigram similarity score, geocoder input address trigram similarity score, coordinates longitude trigram similarity score and coordinates latitude trigram similarity score to classify whether two businesses are identical. Positive examples account for 71% of the data. All of the covariates are outputs from some other models, and are expected to be monotonic. Six and seven of the covariates have missing values. Fax trigram similarity score is missing 97% of the time; phone trigram similarity score is missing 58% of the time; street number trigram similarity score is missing 35% of the time; geocoder input address trigram similarity score is missing 0.1% of the time, and both coordinates longitude trigram similarity score and coordinates latitude trigram similarity score are missing 55% of the time.

With Puzzles data, we use has photo (whether the reviews has a photo), is amazon (whether the reviews were on Amazon), number of times users found the reviews to be helpful, total number of reviews, age of the reviews and number of words in the reviews to classify whether the units sold for the respective puzzle is above 45. The cutoff results in positive label proportions of 49% in the support set, and 51% in the query set. Most of the covariates have unknown monotonicity in their effect in the label.

The 20 OpenML binary classification datasets we used in the numerical studies are listed in Table 9. The 8 multiclass classification datasets are listed in Table 10.

D Description of Numerical Studies

Numerical studies are done with TensorFlow 2 library, ran on the Ubuntu operating system. All training are done on CPU, with 128 GB memory. PLF functions are implemented in the TensorFlow Lattice 1.0 library. In numerical studies, we fixed the random seed to be 91620. Code of numerical studies will be open-sourced upon the acceptance of this work.

Data Name	OpenML ID	# Fine-Tune	# Test	# Features	# Classes
BNG Glass	265	50	137731	10	7
BNG Vehicle	268	50	999950	19	4
BNG Page-Blocks	259	50	295195	11	5
Cars1	40700	50	342	8	3
CPMP 2015	41919	50	477	23	4
AutoUniv	1553	50	650	13	3
Vertebra Column	1523	50	260	7	3
Wall Robot Navigation	1526	50	5406	5	4

Table 10: List of statistics of 8 OpenML multiclass classification datasets used in numerical studies.

In the ablation study of the dependency order r , we used the same DEN architecture as described in Appendix B. For cases with $r \neq 0$, to avoid exponential growth of the number of r-index sets in the classification block, we randomly selected $[d]^2$ r-index sets to be used in the classification network (3).